

miRNA profiling of esophageal adenocarcinoma using transcriptome analysis

Ryan Corlett^{a,1}, Charles Button^{a,1}, Sydney Scheel^{a,1}, Swati Agrawal^a, Vikrant Rai^{b,2} and Kalyana C. Nandipati^{a,2,*}

^aDepartment of Surgery, Creighton University School of Medicine, Omaha, NE, USA

^bDepartment of Translational Research, Western University of Health Sciences, Pomona, CA, USA

Received 28 April 2023

Accepted 4 December 2023

Abstract. Esophageal adenocarcinoma (EAC) occurs following a series of histological changes through epithelial-mesenchymal transition (EMT). A variable expression of normal and aberrant genes in the tissue can contribute to the development of EAC through the activation or inhibition of critical molecular signaling pathways. Gene expression is regulated by various regulatory factors, including transcription factors and microRNAs (miRs). The exact profile of miRs associated with the pathogenesis of EAC is largely unknown, though some candidate miRNAs have been reported in the literature. To identify the unique miR profile associated with EAC, we compared normal esophageal tissue to EAC tissue using bulk RNA sequencing. RNA sequence data was verified using qPCR of 18 selected genes. Fourteen were confirmed as being upregulated, which include *CDH11*, *PCOLCE*, *SULF1*, *GJA4*, *LUM*, *CDH6*, *GNA12*, *F2RL2*, *CTSZ*, *TYROBP*, and *KDELR3* as well as the downregulation of *UGT1A1*. We then conducted Ingenuity Pathway Analysis (IPA) to analyze for novel miR-gene relationships through Causal Network Analysis and Upstream Regulator Analysis. We identified 46 miRs that were aberrantly expressed in EAC compared to control tissues. In EAC tissues, seven miRs were associated with activated networks, while 39 miRs were associated with inhibited networks. The miR-gene relationships identified provide novel insights into potentially oncogenic molecular pathways and genes associated with carcinogenesis in esophageal tissue. Our results revealed a distinct miR profile associated with dysregulated genes. The miRs and genes identified in this study may be used in the future as biomarkers and serve as potential therapeutic targets in EAC.

Keywords: Esophageal adenocarcinoma, RNA sequencing, microRNA, therapeutic target, biomarkers, hub gene

1. Background

Esophageal cancer is the eighth most common cancer and represents the sixth most common cause of cancer mortality globally [1,2]. In the United States, The American Cancer Society estimates about 21,560 new diagnoses and 16,120 deaths related to esophageal cancer in 2023, each with a male predominance [3]. Approximately 10% of esophageal cancers in Western countries are identified to be esophageal adenocarci-

noma (EAC). Further, the incidence of EAC has increased each decade from 1973 to 2015 in the United States, possibly due to the increasing prevalence of EAC risk factors, including obesity and GERD [4]. As incidence increases, the 5-year survival rate remains poor at around 20%, reflecting a need for the development of markers for early diagnosis and better treatment and prevention strategies [5,6,7]. For these reasons, it is essential to identify novel biomarkers and potential therapeutic targets.

Dysregulation of gene transcription has been identified as a critical mechanism underlying cancer pathophysiology [8]. One way that gene transcription is regulated is through microRNA (miR) [9,10]. miRs are highly conserved, single-stranded RNA molecules averaging 22 nucleotides in length that regulate gene expression by binding target messenger RNA (mRNA).

¹Contributed equally to this manuscript.

²These authors jointly supervised the work.

*Corresponding author: Kalyana C. Nandipati, Esophageal Center CHI Health Creighton University Medical Center-Bergan Mercy 7710 Mercy Road, Suite 501, Omaha, NE 68124, USA. Tel.: +1 402 280 5292; Fax: +1 402 280 5979; E-mail: kcn62720@creighton.edu.

In general, miR-mRNA binding suppresses the mRNA molecule's translation and/or degradation, leading to increased or decreased expression of certain genes [11, 12]. miRs may therefore possess either tumor-promoting (onco-miR) or suppressing activity based on the deactivated target mRNA [11]. Dysregulated miRs have been associated with many cancer phenotypes and implicated in a variety of dysregulated cellular pathways and mechanisms, including in EAC [13,14,15,16]. While not all dysregulated genes and molecular pathways lead consistently to carcinogenesis, a variety of mechanisms have been described in EAC development [17]. Furthermore, relatively few miRs have been reported to be associated with EAC, which necessitates further investigation into possible miRs associated with EAC development [18,19,20,21,22].

2. Objective

This study aims to identify novel miRs associated with EAC and their potential gene targets.

3. Methods

3.1. Patient selection

The protocol for this prospective study was approved by the Institutional Review Board (IRB# 1194896) of Creighton University. All patients undergoing primary endoscopic biopsy or surgical resection of suspected EAC were considered for inclusion in this study. A written informed consent was obtained from all patients scheduled for surgery at Creighton University Medical Center. For this study, ~ 2 mm tissue samples were collected from the EAC lesion. A similar-sized biopsy was taken from adjacent normal tissue at the time of the initial biopsy to serve as a control. Inclusion criteria included all patients willing to participate with a diagnosis of EAC. Patients unwilling to participate and patients less than 19 years of age were excluded from the study. Patient selection and inclusion in this study conform with The Code of Ethics of the World Medical Association (Declaration of Helsinki).

3.2. Tissue collection and processing

The EAC and normal tissue collected during surgical endoscopy or resection were transported to the lab the same day at 4°C and processed for total RNA

isolation. Total RNA was isolated using TRI reagent (TRIzol™ Reagent, Sigma, Catalog #T9424, St. Louis, Missouri, USA) following the manufacturer's guidelines. Total RNA yield was measured using NanoDrop One (Thermo Fisher Scientific Inc.) and 1 µg of total RNA was sent for bulk RNA sequencing. The RNA samples with RNA integrity number (RIN) > 6 were subjected to sequencing. Sequencing was performed on a total of 4 control and 4 EAC samples. The extracted RNA was also used to prepare cDNA.

3.3. Bulk RNA sequencing and analysis

We conducted bulk RNA sequencing on 4 EAC and 4 normal esophageal mucosa samples. Genetic analysis and statistical inference were performed at The University of Nebraska Medical Center (UNMC) using the following protocol: The original fastq format reads were trimmed by the fqtrim tool (<https://ccb.jhu.edu/software/fqtrim>) to remove adapters, terminal unknown bases (Ns), and low quality 3' regions (Phred score < 30). The trimmed fastq files were processed by FastQC [23]. The trimmed fastq files were then processed by the UNMC standard pipelines utilizing STAR [24] as the aligner and RSEM [25] as the tool for annotation and quantification at both gene and isoform levels. The trimmed fastq files were mapped to the hg38 human reference genome (GRCh38). The normalized expression abundance in TPM (Transcripts Per Kilobase Million) and FPKM (Fragments Per Kilobase of Transcript Per Million mapped reads) values for all the available genes and isoforms were analyzed. The TPM values were used for further analysis. To calculate statistically significant differences in gene expression in EAC tissue compared to normal tissue, a Student's *t*-test was used for all the available genes using TPM values. The Benjamini-Hochberg adjusted *p*-values [26] were also analyzed to adjust for multiple-testing caused false discovery rate (FDR).

3.4. Identification of differentially expressed genes (DEGs)

Genes were filtered using $|\log_{2}FC| \geq 2$ and $p \leq 0.05$ as cutoffs to determine significant upregulation/downregulation. Fold change and *p*-value were measured against normal epithelium, which we considered to have normal expression of each gene. Genes with a positive log₂FC were considered upregulated. Genes with a negative log₂FC were considered downregulated. Genes that met these criteria were desig-

nated as differentially expressed genes (DEGs). A volcano plot of gene screening was constructed using Prism GraphPad Software (San Diego, California, USA, www.graphpad.com).

3.5. Ingenuity pathway analysis

To investigate the potentially novel miR-gene interactions associated with the DEGs identified through bulk RNA sequencing, we conducted Ingenuity Pathway Analysis (IPA). IPA is a bioinformatic analysis platform created by QIAGEN Inc. that predicts functional relationships among sets of genes. Within IPA, we further utilized Causal Network and Upstream Regulator Analyses. (QIAGEN Inc. <https://digitalinsights.qiagen.com/products-overview/discovery-insights-portfolio/analysis-and-visualization/qiagen-ipa/>). These analytical tools allow for exploration beyond direct relationships and provide insight into potential physiologic mechanisms that are associated with target datasets. Causal Network Analysis uses experimental data to predict regulatory species, including miRs and transcription factors that are not directly connected to DEGs. Upstream Regulator Analysis predicts regulatory molecules that influence the observed genotype associated with input data through either upstream or downstream changes to gene transcription. Both analysis methods may provide novel insight into pathophysiological mechanisms that control the development of EAC that might not be readily apparent in a set of differentially expressed genes. microRNAs and their associated gene targets were obtained through IPA. Disease and biologic function analysis of IPA is included in Supplemental File 1.

3.6. Protein-protein interaction, functional enrichment, and identification of hub genes

Functional relationship analysis for the DEGs was conducted using the Search Tool for Retrieval of Interacting Genes (STRING), accessed through (<http://string-db.org>). STRING is a web-based database that can predict relationships between input genes to create protein-protein interaction (PPI) networks. Our network was constructed using a confidence of interaction score > 0.4. The PPI was exported to Cytoscape (<https://cytoscape.org/>) for network visualization (Fig. 2).

To further narrow the focus of our investigation, we identified genes involved in the top 10 enriched Gene Ontology (GO) Biological Processes (Table 2). GO

Term false discovery rate < 0.05 was used as a cutoff for identifying significantly enriched terms. Genes within the top 10 GO Terms were isolated and paired with corresponding miR-gene relationships identified through IPA for network visualization. We isolated miR-DEG interactivity into four sub-networks based on analysis type to identify miR-gene connections more clearly: Causal Network Activated, Causal Network Inhibited, Upstream Regulator Activated, and Upstream Regulator Inhibited.

Hub genes demonstrate high connectivity in PPI networks and can help identify genes that play critical roles in underlying network pathways [27]. Therefore, identifying hub genes may provide insight into meaningful biological mechanisms involved in PPI networks and assist in clarifying the importance of an underlying gene in disease development. We used the Cytoscape plugin cytoHubba [28] to identify hub genes within our PPI. Within cytoHubba, we conducted hub analysis to determine the 20 top hub genes using five commonly used embedded algorithms, which include Maximal Clique Centrality (MCC), Maximum Neighborhood Component (MNC), Density of Maximum Neighborhood Component (DMNC), Degree method (Degree), and Edge Percolated Component (EPC) [29]. We further conducted Molecular Complex Detection (MCODE) within Cytoscape, a separate Cytoscape plugin that assists in identifying highly connected hub genes in large PPIs [30]. MCODE was analyzed using a Network Scoring degree cutoff of 2, and cluster finding was set to 'haircut' utilizing a node score cutoff of 0.2, K-Core of 2, and a maximum depth of 100. MCODE output modules were considered significant with a k-score > 4.0.

3.7. qPCR of DEGs for RNA sequencing validation

To verify the data identified with RNA sequencing, qPCR (real-time polymerase chain reaction) was used to quantify the expression of 18 DEGs identified through IPA analysis. 13 previously unreported DEGs (*PCOLCE*, *CDH11*, *GJA4*, *PTGFR*, *CDH6*, *LUM*, *GNA12*, *SULF1*, *CDC14B*, *KDEL3*, *TYROBP*, *UGT1A1*, and *F2RL2*) were selected based on literature review into each gene's known functional relationships related to mechanisms involved in EAC risk and development, including inflammatory signaling, cellular organization, and mechanisms involved in insulin signaling. The remaining five genes (*FOXF1*, *IGFBP7*, *CTRH1*, *HEYL*, and *NFATC2*) have been previously characterized in relation to EAC and were analyzed

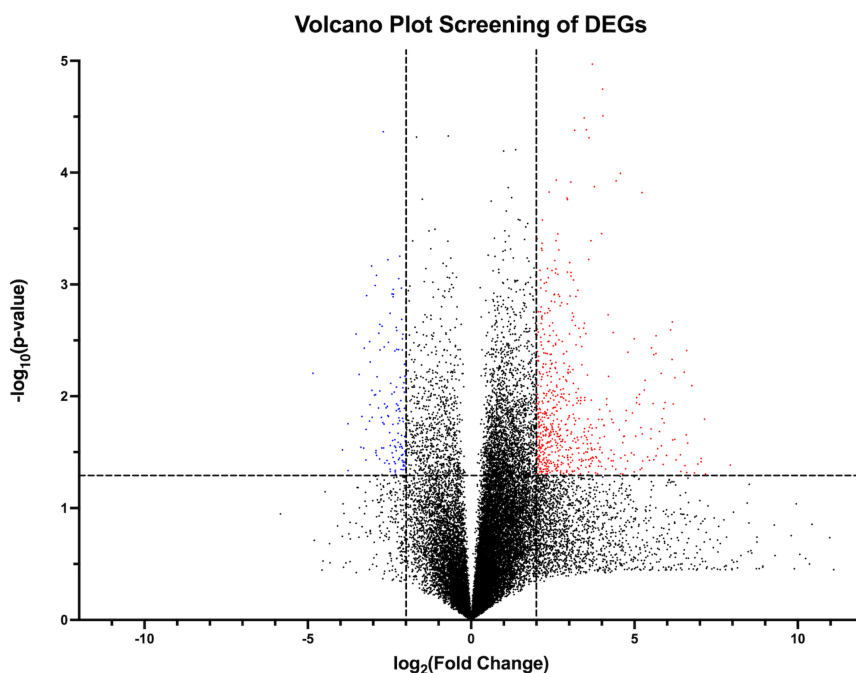


Fig. 1. Volcano plot visual representation of filtering out candidate DEGs from RNA sequence data using $|\log_2\text{FC}| \geq 2$ (vertical dotted lines) and $p \leq 0.05$ (horizontal dotted line) as cutoff values. (Red – Upregulated DEGs; Blue – Downregulated DEGs; Black – Did not fulfill inclusion criteria.)

for additional validation. Of the selected genes, seven were identified as highly connected hubs and therefore serve as potentially important targets for future research: *PCOLCE*, *CDH11*, *GJA4*, *PTGFR*, *CDH6*, *LUM*, *SULF1*, and *TYROBP*.

Total RNA was extracted using the TRIZOL method (T9424, Millipore Sigma, Burlington, Massachusetts, USA) following standard protocol in our laboratory. The yield of total RNA was quantified using Nanodrop 2000 Spectrophotometer (Thermo Fisher Scientific, Waltham, Massachusetts, USA). Following this, 2 μg cDNA was prepared using AzuraQuant™ cDNA Synthesis Kit (AZ-1996, Raynham, Massachusetts, USA) following the manufacturer's instructions. qRT-PCR was done in triplicate for the selected genes using AzuraView™ GreenFast qPCR Blue Mix HR (AZ-2420, Raynham, Massachusetts, USA) with PCR cycling of 5 min at 95°C for initial denaturation then 40 cycles consisting of 30 seconds at 95°C (denaturation), 30 seconds at 55–60°C, and 30 seconds at 72°C (extension) followed by melting curve analysis. A total of three replicates were produced, and an average expression was used for further analysis. Fold changes in mRNA expression relative to controls were analyzed using the $2^{-\Delta\Delta\text{CT}}$ method after normalization with β -actin. The primers for selected genes (Table 1) were ob-

tained from Integrated DNA Technologies (Coralville, Iowa, USA). Normalized qPCR expression was graphed using Prism GraphPad, and cycle threshold (CT) values are available in Supplemental File 1.

4. Results

4.1. RNA sequencing and differentially expressed genes

RNA sequencing data revealed a total of 58,826 detected genes. Of these, 784 genes met our criteria for significantly upregulated or downregulated ($|\log_2\text{FC}| \geq 2$ and $p \leq 0.05$). The total of upregulated gene transcripts was equal to 644, and the total of downregulated genes was equivalent to 140. A visual representation of candidate gene selection is shown in the volcano plot (Fig. 1). The complete list of genes from our RNA sequencing data can be accessed through Supplemental File 1. Of the detected genes, 196 were found to be long non-coding RNA, immunoglobulins, and novel transcripts and were removed for further analysis ($n = 131$ upregulated; $n = 65$ downregulated). The remaining 588 differentially expressed genes were used for further network analysis and contained 513 upregulated and 75 downregulated genes.

Table 1
Primer sequences used to perform qPCR on selected DEGs detected using RNA sequencing analysis

Gene Name	Symbol	Sequence 5' → 3' (Forward)	Sequence 5' → 3' (Reverse)
Cadherin 11	CDH11	TGGCAGCAAGTATCCAAATGG	TTTGGTTACGTGTAGGCAC
Procollagen C-endopeptidase enhancer 1	PCOLCE	GTGCGGAGGGATGTGAAG	CGAAGACTCGGAATGAGAGGG
Sulfatase 1	SULF1	GGACGGATACAGCAGGAACG	CAGCACATGGGTGTAGTCACA
Gap junction alpha-4 protein	GJA4	TGCAAGAGTGTGCTAGAGGC	ACA AAGCAGTCCACGAGGTAG
Lumican	LUM	TAACTGCCCTGAAAGCTACCC	GGAGGCACCATTTGTACACTT
Cadherin 6	CDH6	AGA AACTTACCGCTACTTCTTGC	TGCCACATACTGATAATCGGA
Guanine nucleotide-binding protein subunit alpha-12	GNA12	GGAGGGATTCTGGCATCAGG	CCGATCCGGTCCAAGTTGTC
Prostaglandin F2-alpha receptor	PTGFR	AAGTCCAAGGCATCGTTTCTG	TGACTCCAATACACCGCTCAAT
Guanylate cyclase 1, soluble, alpha 3	GUCY1A1	GGGACCAGATTAGATGGTGACTTGG	CCCATCATGCTGTTCCTATGTG
Coagulation factor II (thrombin) receptor-like 2	F2RL2	GCAAAGCCAACCTTACCCATT	GAGGTAGATGGCAGGTATCAGT
Cathepsin Z	CTSZ	GTGCAGAACGTCAATCGACTG	TTGCAGGTCTCGTCAGGGA
TYRO protein tyrosine kinase-binding protein	TYROBP	ACTGAGACCGAGTCGCCTTAT	ATACGGCCTCTGTGTGTGAG
Dual specificity protein phosphatase CDC14B	CDC14B	GCCATTCTTACAGCAGACCA	TGTAAACCAATGGCAGATTGAGT
ER lumen protein-retaining receptor 3	KDEL3	TCCCAGTCAITGGCCTTTCC	CCAGTTAGCCAGGTAGAGTGC
UDP glucuronosyltransferase family 1 member A1	UGT1A1	TTGTCTGGCTGTTCCCACTTA	GGTCCGTCAGCATGACATCA
Insulin-like growth factor-binding protein 7	IGFBP7	CGAGCAAGTCCCTTCCATAGT	GGTGTCCGGGATTCGGATGAC
Forkhead box protein F1	FOXF1	CCCAGCATGTGTACCCGAAA	ATCACGCCAAGGCTTGTGTCT
Collagen triple helix repeat-containing protein 1	CTHR1	CAATGGCATTCGGGGTACAC	GTACACTCCGCAATTTTCCCAA
Nuclear factor of activated T-cells, cytoplasmic 2	NFATC2	GAGCCGAATGCACATAAGGTC	CCAGAGAGACTAGCAAGGGG
Hairy/enhancer-of-split related with YRPW motif-like protein	HEYL	GGAAGAAACGCAGAGGGATCA	CAAGCGTCCGCAATTCAGAAAAG

Protein-Protein Interaction Network of Differentially Expressed Genes

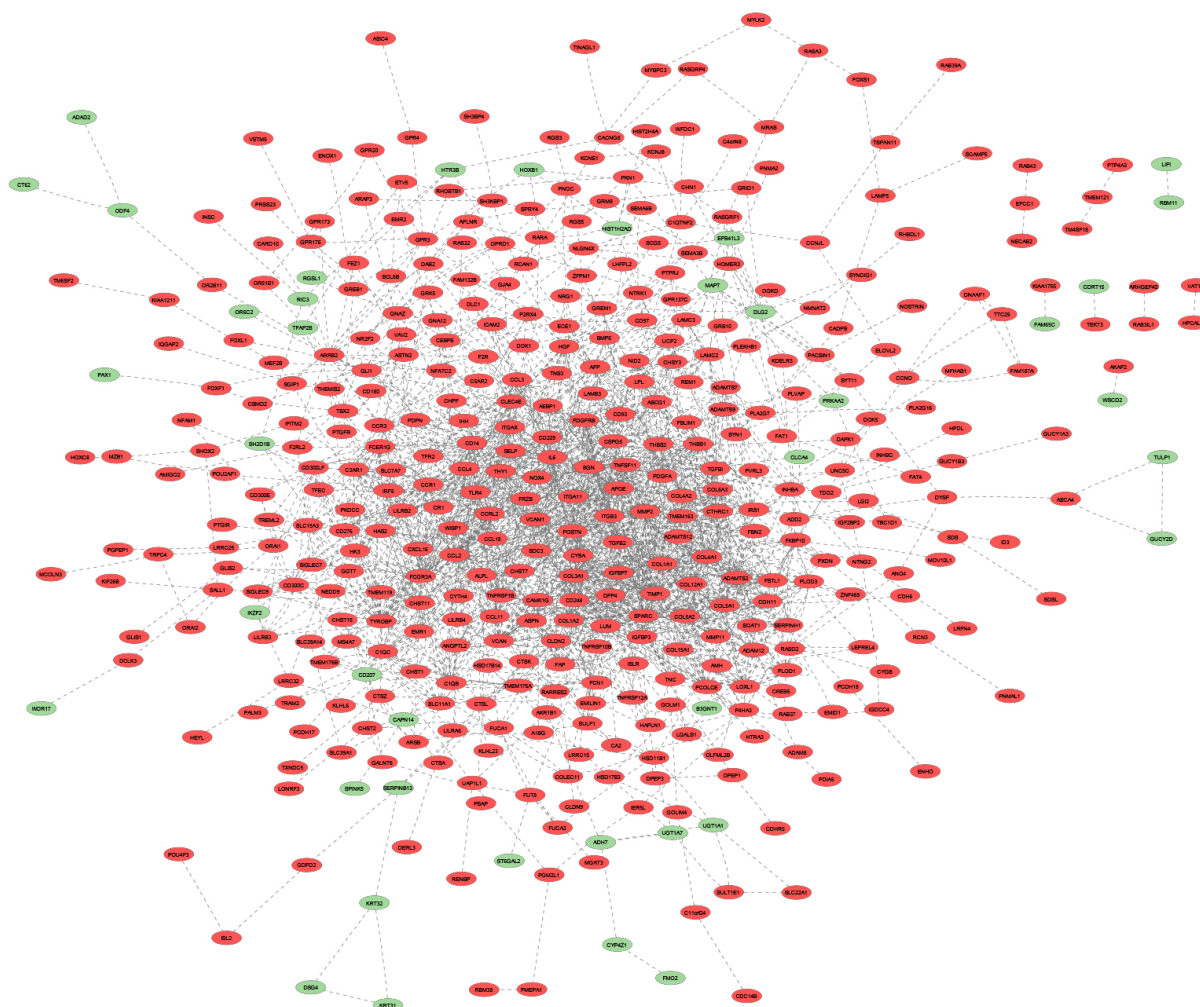


Fig. 2. PPI among DEGs identified using RNA-sequencing analysis (Red-Upregulated DEG; Green-Downregulated DEG; Grey line-Predicted connection between adjacent genes).

4.2. Protein-protein interaction

A protein-protein interaction map of the 588 DEGs was created using STRING that included 526 mappable nodes and displayed 2085 edges (expected number of edges = 789, enrichment p -value = $< 1.0 \times 10^{-16}$). A detailed representation of the PPI network was constructed using Cytoscape and is displayed in Fig. 2.

4.3. Gene enrichment

GO Biological Process enrichment of the obtained PPI network revealed 156 significantly overrepresented genes from pathways involved in cell adhesion, collagen

fibril organization/biosynthesis, inflammatory response, ECM organization, cell migration, positive regulation of ERK1/2 cascade, osteoblast differentiation, and cell-to-cell signaling (Table 2). The top 10 GO Terms were ranked by significance using $-\log_{10}(p\text{-value})$ and are displayed in Fig. 3. The 156 genes found within each of the top 10 most significantly enriched GO Terms are mapped in Fig. 4A and B.

4.4. Hub gene analysis

Hub gene analysis revealed 84 unique hub genes using cytoHubba and MCODE modules. Of these, cytoHubba produced 48 genes across all five analysis

Table 2
Top 10 enriched GO Terms Biological Process used to filter genes into relevant biological processes pertaining to EAC

Top 10 Gene Ontology Terms Used for miR-Gene Inference			
Accession ID	Gene Ontology Term	p-value	# of DEGs
GO:0007155	Cell adhesion	3.30E-26	67
GO:0030199	Collagen fibril organization	1.10E-16	22
GO:0006954	Inflammatory response	2.10E-10	37
GO:0030198	Extracellular matrix organization	2.70E-10	24
GO:0032964	Collagen biosynthetic process	4.50E-08	7
GO:0016477	Cell migration	1.20E-07	25
GO:0070374	Positive regulation of ERK1 and ERK2 cascade	9.80E-07	21
GO:0030335	Positive regulation of cell migration	2.80E-06	22
GO:0001649	Osteoblast differentiation	3.50E-06	15
GO:0007267	Cell-cell signaling	5.40E-06	20

-log₁₀(p-value) of Top 10 Enriched Gene Ontology Terms

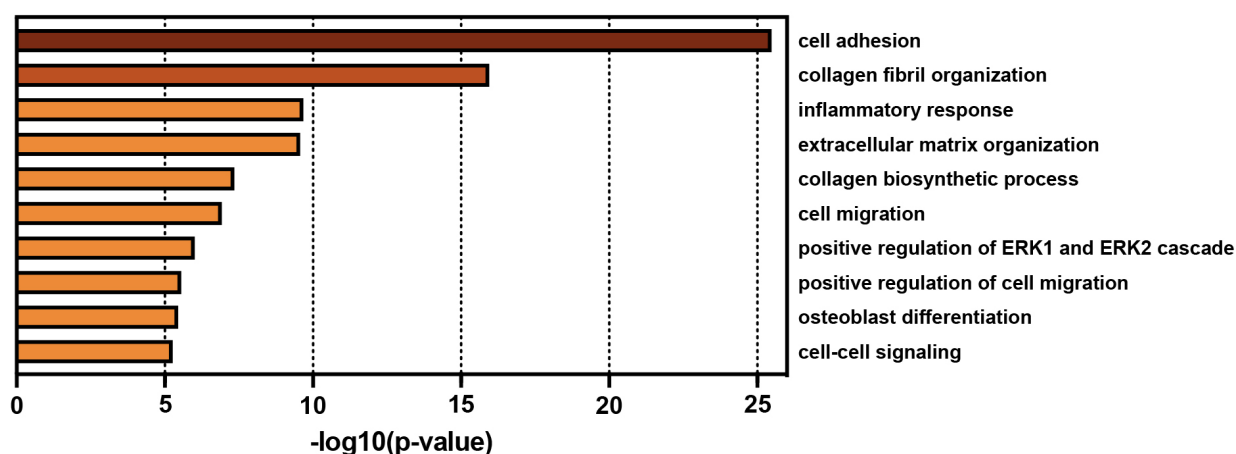


Fig. 3. Top 10 enriched GO Terms Biological Process used to filter genes into relevant biological processes pertaining to EAC.

methods (MCC, MNC, Degree, EPC, and DMNC), displayed in Fig. 5A. MCODE revealed 68 genes across four significant modules, depicted in Fig. 5B. Combined, 32 genes demonstrated overlap and appeared in both analysis methods (Fig. 5C). From cytoHubba, no genes were found across all five algorithms of analysis. Despite this, nine genes were found to overlap between MCC, MNC, Degree, and EPC methods (*MMP2*, *BGN*, *COL1A2*, *COL1A3*, *VCAN*, *THBS1*, *COL1A1*, *POSTN*, and *TIMP1*). An additional nine genes were found within three separate algorithmic outputs (*COL5A1*, *COL4A1*, *COL5A2*, *THBS2*, *COL6A3*, *LUM*, *ITGB3*, *CCL2*, and *IL6*).

MCODE analysis of the PPI revealed four significant modules. The most significant module, Module 1, contained 27 nodes and 271 edges (k-score = 20.846). Module 2 contained 21 nodes with 79 edges 9 (k-score = 7.900), Module 3 contained 15 nodes with 49 edges (k-score = 7.000, and Module 4 contained five nodes

with ten edges (k-score 5.000). As expected in MCODE analysis, no genes overlapped between modules. The four significant MCODE modules were mapped onto the complete PPI network in Fig. 5D.

4.5. miRs

Ingenuity Pathway Analysis of our samples demonstrated the presence of both activated and inhibited networks. Causal network analysis revealed 33 total miRNA; 6 associated with activated networks (mir-28, miR-145-5p, mir-19, mir-221, miR-133a-3p, and mir-24) and 27 associated with inhibited networks (miR-149-5p, miR-96-5p, miR-204-5p, miR-335-3p, miR-30c-5p, miR-338-3p, mir-10, mir-30, mir-630, miR-30c-5p, mir-338, miR-450a-5p, miR-29b-3p, miR-2392, Mir200, mir-128, let-7a-5p, mir-1, miR-124-3p, let-7, miR-219a-5p, miR-218-5p, mir-182, miR-491-5p, MIR100-LET7A2-MIR125B1, MIR17HG, MIR99A-

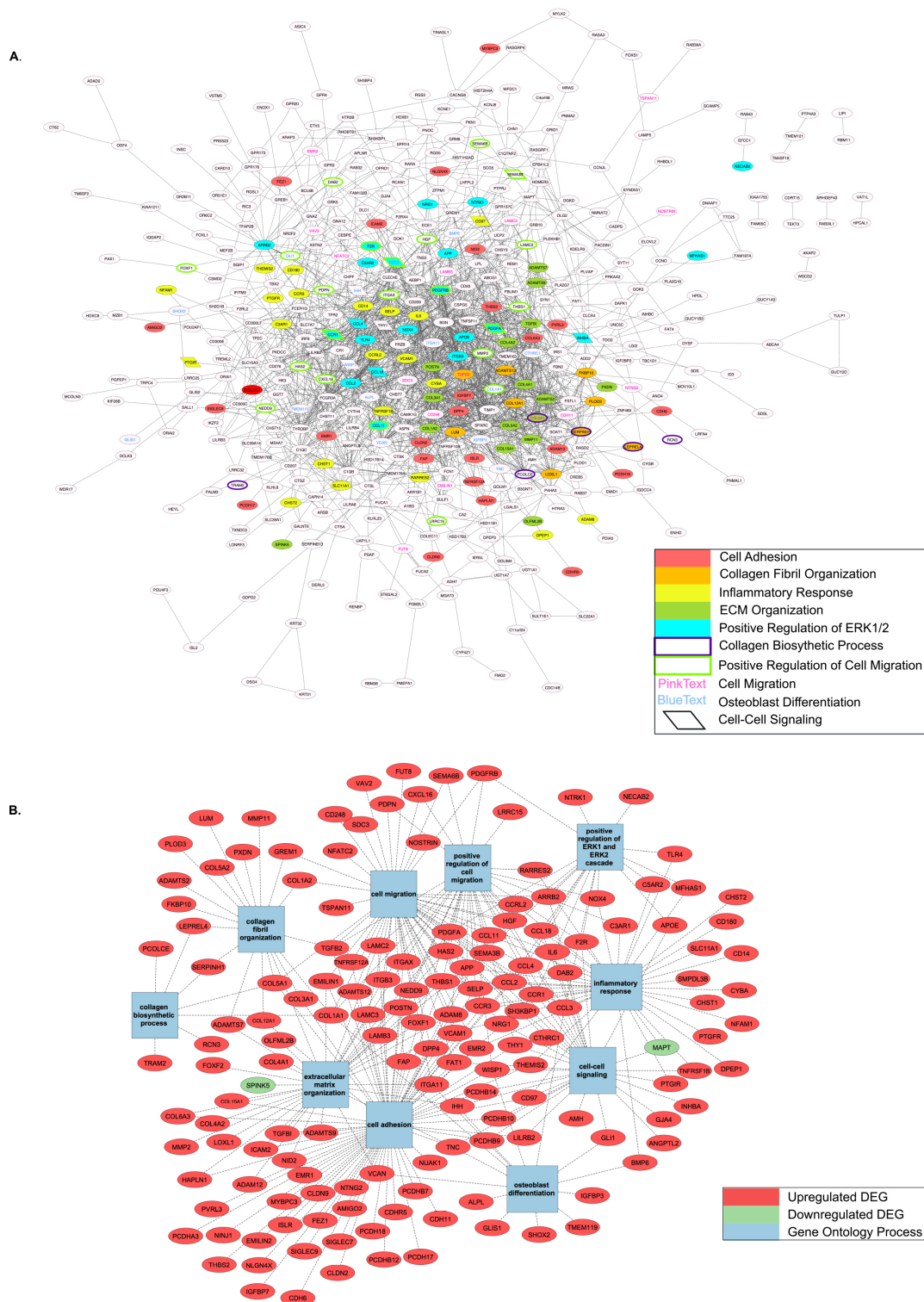


Fig. 4. PPI networks with Top 10 enriched GO Terms by Biological Process. A) Complete PPI network with Top 10 GO Terms highlighted based on gene inclusion; B) Genes found within Top 10 GO Terms and mapped individually to involved process.

Hub Gene Identification

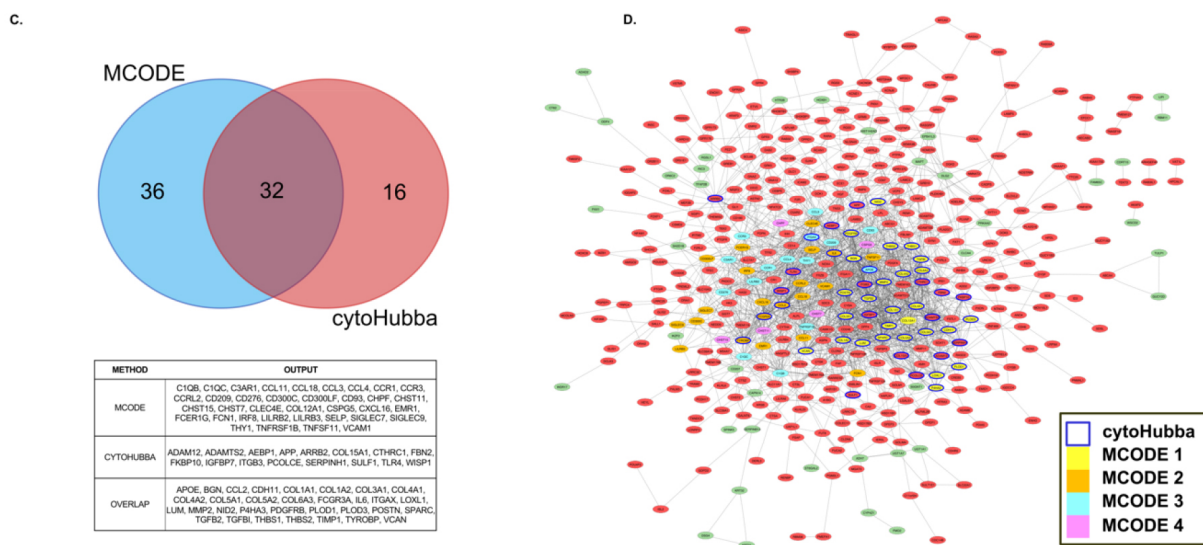
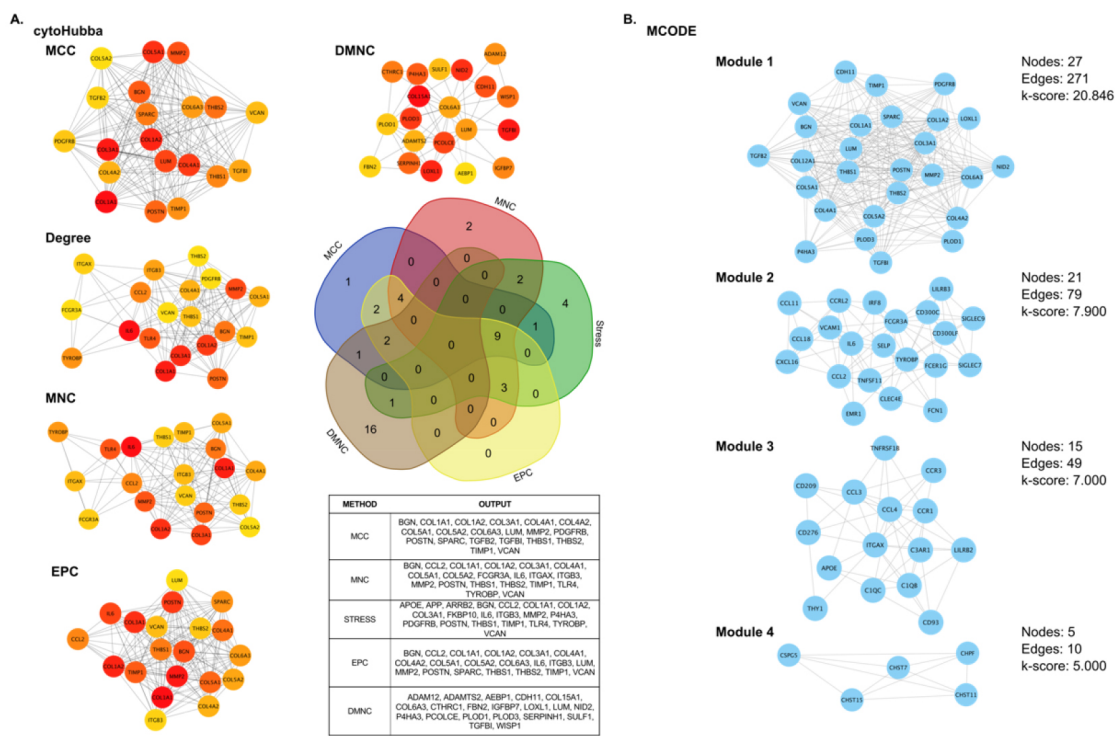


Fig. 5. Hub gene analysis of significantly dysregulated genes using cytoHubba and MCODE plugins for Cytoscape. A) Outcome of cytoHubba analysis (using MCC, Degree, MNC, EPC, and DMNC algorithms) compared for overlap using five-way Venn diagram; B) Significant ($k\text{-score} > 4.0$) MCODE modules; C) Comparative analysis of genes identified using cytoHubba and MCODE analyses D) PPI of DEGs with identified hub genes highlighted. Purple outlined nodes: DEGs identified as hubs using cytoHubba, yellow nodes: identified in MCODE module 1, orange nodes identified in MCODE module 2, sky blue nodes: identified in MCODE module 3, pink nodes: identified in MCODE module 4, dotted line: predicted gene-gene interaction from STRING enrichment.

Table 3a

Identified miRs in activated networks indicated through Causal Network analysis (esophageal adenocarcinoma vs. healthy adjacent tissue). miR-DEG targets are divided into upregulated ($\log_2 FC > 2$, $p < 0.05$) and downregulated ($\log_2 FC < 2$, $p < 0.05$)

Activated Causal Network miR-DEG Relationships		
ASSOCIATED WITH ACTIVATED NETWORK	DEGS ($\log_2 > 2$, $p < 0.05$)	DEGS ($\log_2 < -2$, $p < 0.05$)
miR-28	ADAMTS9, ADGRE5, ALPL, ANGPTL2, ARRB2, BMP6, C3AR1, CCN4, CCR1, CCR3, CD14, CLDN2, COL12A1, COL1A2, CXCL16, CYBA, DAB2, DPEP1, DPP4, EMILIN1, FAP, FAT1, FEZ1, FOXF2, GREM1, ICAM2, INHBA, ITGAX, ITGB3, LUM, MFHAS1, MMP2, NECTIN3, NFAM1, NFATC2, NID2, NLGN4X, NRG1, NTRK1, PCDH17, PCDHB14, PCOLCE, PDGFRB, POSTN, RARRES2, SELP, SEMA3B, SERPINH1, SH3KBP1, SHOX2, TGFB1, THBS2, TNFRSF12A, VCAM1	SPINK5
miR-145-5p	ADAM12, ADAMTS12, ADAMTS2, ADAMTS9, ADGRE2, ADGRE5, AMH, ANGPTL2, APOE, APP, ARRB2, BMP6, C3AR1, CCL11, CCL18, CCL2, CCL3, CCL4, CCN4, CCR1, CCR3, CCRL2, CD14, CHST2, CLDN2, COL12A1, COL1A1, COL1A2, COL3A1, COL4A1, COL4A2, COL5A1, COL6A3, CYBA, DAB2, DPEP1, EMILIN1, FAP, FAT1, FOXF2, FUT8, GJA4, GLI1, GREM1, HAS2, HGF, IGFBP3, IGFBP7, IL6, INHBA, ITGA11, ITGAX, ITGB3, LAMB3, LAMC2, LOXL1, MFHAS1, MMP11, MMP2, NECTIN3, NEDD9, NFAM1, NFATC2, NID2, NIN1, NOX4, NRG1, PCDH17, PCDHB12, PCDHB14, PCDHB7, PDGFA, PDGFRB, PDPN, POSTN, PTGFR, PXDN, RARRES2, RCN3, SDC3, SELP, SEMA3B, SERPINH1, SHOX2, SLC11A1, SMPDL3B, TGFB1, THBS1, THBS2, THY1, TLR4, TNC, TNFRSF12A, VCAM1, VCAN	SPINK5
miR-19	ADAMTS2, AMH, AMIGO2, ANGPTL2, APOE, C3AR1, CCL11, CCL18, CCL2, CCL4, CCR1, CCR3, CCRL2, CD180, CD248, CLDN2, COL12A1, COL15A1, COL1A1, COL1A2, COL3A1, COL5A2, CTHRC1, CYBA, DAB2, DPP4, EMILIN2, FAP, FKBP10, FUT8, GLIS1, GREM1, HAPLN1, HAS2, HGF, IGFBP3, IHH, IL6, LAMB3, LOXL1, LRRC15, MFHAS1, MMP2, NFATC2, NLGN4X, NOX4, NRG1, PCDH18, PCDHB14, PDGFRB, PLOD3, PTGFR, RARRES2, SDC3, SEMA3B, TGFB2, THBS1, TMEM119, TNFRSF1B, VCAM1	MAPT
miR-221	ADAM8, ADAMTS9, ADGRE1, ADGRE2, ADGRE5, AMH, AMIGO2, ANGPTL2, APP, ARRB2, CCL18, CCL2, CD14, CD248, CDHR5, CLDN2, COL12A1, COL3A1, CTHRC1, CYBA, DPEP1, DPP4, EMILIN1, EMILIN2, FAP, FAT1, FOXF2, GLI1, HAPLN1, ICAM2, IHH, IL6, LAMB3, LAMC2, LOXL1, LRRC15, MFHAS1, MMP11, MMP2, NECTIN3, NFAM1, NLGN4X, NOSTRIN, NOX4, NRG1, PCDH17, PCDHB14, PDPN, PLOD3, PXDN, RCN3, SDC3, SELP, SEMA3B, SH3KBP1, SHOX2, SLC11A1, TGFB1, THBS1, THBS2, TNC, VCAM1, VCAN	
miR-133a-3p	ALPL, CCL11, CCL2, CCL3, CCL4, CCN4, COL1A1, COL3A1, COL4A1, HAS2, IGFBP3, IL6, ITGB3, MMP2, PCOLCE, PDGFRB, POSTN, SHOX2, TGFB2, THBS1, THBS2, VCAN	MAPT
miR-24	ALPL, CCL11, CCL2, CCL3, CCL4, CCN4, COL1A1, COL3A1, HAS2, IGFBP3, IL6, ITGB3, MMP2, NOX4, POSTN, VCAN	MAPT

LET7C-MIR125B2, and MIRLET7). Upstream Regulator Analysis revealed 24 total miRNA; one was associated with activated networks (miR-223) and 23 were associated with inhibited networks (miR-335-3p, miR-338-3p, miR-30c-5p, miR-450a-5p, miR-29b-3p, miR-2392, let-7a-5p, miR-124-3p, miR-1, let-7, miR-29, miR-182, miR-199a-5p, miR-1-3p, miR-125b-5p, miR-27a-3p, mir-193, miR-155-5p, miR-291a-3p, miR-205-5p, miR-296-5p, miR-8, and miR-146). All miRs were associated with DEGs within the complete dataset. The miR-DEG relationships identified through Causal Network Analysis are displayed in Table 3a and 3b and Fig. 6A and 6B. Relationships obtained through Up-

stream Regulator Analysis are depicted in Table 4a and 4b and Fig. 6C and 6D. The complete list of gene targets identified using IPA can be found in Supplemental File 1.

We thoroughly reviewed the literature and found 18 miRs previously described in relation to EAC compared to normal epithelium. These include let-7, miR-1-3p, miR-145-5p, miR-149-5p, miR-199a-5p, miR-27a-3p, MIR200, miR-221, miR-223, miR-335-3p, miR-338-3p, miR-133a-3p, miR-30c-5p, miR-630, MIR17HG, MIR99A-LET7C-MIR125B2, and MIRLET [22,31,32, 33,34,35,36,37,38,39,40,41,42]. In addition, mir-218-5p has been described to be elevated in the serum of

Table 3b

Identified miRs in inactivated networks indicated through Causal Network analysis (esophageal adenocarcinoma vs. healthy adjacent tissue). miR-DEG targets are divided into upregulated ($\log_2 FC > 2$, $p < 0.05$) and downregulated ($\log_2 FC < 2$, $p < 0.05$)

Inactivated Causal Network miR-DEG Relationships		
ASSOCIATED WITH IN-ACTIVATED NETWORK	DEGS ($\log_2 > 2$, $p < 0.05$)	DEGS ($\log_2 < -2$, $p < 0.05$)
miR-149-5p	ADAM12, ADAMTS9, ADGRE5, ALPL, AMH, AMIGO2, ANGPTL2, ARRB2, BMP6, CCL2, CCN4, CCR1, CD14, CDH11, CDH6, CHST2, CLDN2, COL15A1, CTHRC1, CYBA, DAB2, DPP4, EMILIN1, FAP, FEZ1, FOXF1, FOXF2, FUT8, GLI1, GLIS1, GREM1, HAPLN1, ICAM2, IHH, IL6, INHBA, ITGB3, LAMC2, LUM, MFHAS1, NEDD9, NINJ1, NLGN4X, NRG1, PCDH17, PCDH18, PCDHB14, PDGFRB, PTGFR, SEMA3B, SLC11A1, SMPDL3B, TGFB2, TGFB1, THBS2, TNC, VAV2, VCAM1	SPINK5
miR-96-5p	ADAM12, ADAMTS9, ALPL, AMIGO2, APOE, APP, ARRB2, CCL2, CCN4, CCR1, CCRL2, CDH11, CLDN2, COL12A1, COL1A1, COL3A1, COL4A1, COL5A1, CYBA, DPEP1, EMILIN1, F2R, FAT1, FOXF1, FOXF2, GLI1, GREM1, HAS2, HGF, ICAM2, IGFBP7, IHH, INHBA, ITGB3, LAMB3, LAMC2, MFHAS1, MMP2, NECTIN3, NEDD9, NFAM1, NFATC2, NID2, NINJ1, PCDH18, PCDHB14, PCOLCE, PDGFA, PDPN, POSTN, SELP, SERPINH1, TGFB2, TGFB1, THBS1, THY1, TLR4, TNC, TNFRSF12A, VCAN	
miR-204-5p	ADAM12, ADAMTS12, ADAMTS2, ADAMTS9, ANGPTL2, BMP6, C3AR1, CCL18, CCL2, CCL3, CCR3, CD180, CD248, CDH11, CDH6, CHST2, CLDN2, COL12A1, COL15A1, COL1A2, CTHRC1, CYBA, DPEP1, DPP4, F2R, FAP, FOXF2, GLIS1, HAS2, ICAM2, IL6, LAMB3, LOXL1, MFHAS1, MMP11, MMP2, NFATC2, NINJ1, NLGN4X, NOX4, NRG1, NUAK1, PCDH17, PCDHB14, PDGFA, POSTN, PTGFR, PXDN, RARRES2, SEMA3B, SERPINH1, SH3KBP1, SHOX2, SLC11A1, SMPDL3B, TGFB2, TGFB1, THBS2, TMEM119, VAV2, VCAN	
miR-335-3p	ADAMTS2, COL1A1, COL1A2, COL4A1, COL4A2, COL5A1, COL5A2, NID2, PDGFA, VCAN	
miR-30c-5p	ADAM12, ADAMTS2, ADGRE5, APOE, APP, ARRB2, CCL2, CCL4, COL1A1, COL1A2, COL3A1, COL4A1, COL4A2, COL5A1, COL5A2, DPEP1, DPP4, EMILIN1, F2R, FAT1, FOXF1, HAS2, HGF, IGFBP3, IL6, INHBA, LAMC2, NECTIN3, NFAM1, NID2, NINJ1, PDGFA, PDGFRB, SELP, SERPINH1, TGFB2, TGFB1, THBS1, THBS2, THY1, TNC, TNFRSF1B, VCAN	
miR-338-3p	ADAMTS2, COL1A1, COL1A2, COL4A1, COL4A2, COL5A1, COL5A2, NID2, PDGFA, VCAN	
miR-10	ADAM12, ADGRE5, ALPL, APOE, APP, ARRB2, CCL2, CCL3, CCL4, CCN4, CCR1, CCRL2, CLDN2, COL1A2, COL4A1, COL4A2, COL5A2, DPEP1, EMILIN1, F2R, FAT1, FOXF1, GLI1, HGF, IHH, INHBA, ITGB3, LAMB3, LAMC2, NECTIN3, NFAM1, NFATC2, NID2, NINJ1, NOX4, PDGFA, PDGFRB, POSTN, SELP, SERPINH1, TGFB2, TGFB1, THBS1, THY1, TNFRSF1B	
miR-30	ADAM12, ADAMTS9, ADGRE5, APOE, APP, ARRB2, CCL11, CCL3, COL1A1, COL3A1, COL4A1, COL4A2, COL5A2, DPEP1, DPP4, EMILIN1, F2R, FAT1, FOXF1, HAS2, HGF, IGFBP3, IL6, INHBA, ITGB3, LAMC2, MFHAS1, MMP2, NECTIN3, NFAM1, NFATC2, NID2, NINJ1, PDGFA, PDGFRB, POSTN, SELP, SERPINH1, TGFB2, TGFB1, THBS1, THBS2, THY1, TNC, TNFRSF1B, VCAM1, VCAN	
miR-630	ADAM12, ADGRE5, APOE, APP, ARRB2, CCL2, CCL4, COL1A1, COL3A1, COL4A1, COL4A2, COL5A2, DPEP1, DPP4, EMILIN1, F2R, FAT1, FOXF1, HAS2, HGF, IGFBP3, INHBA, LAMC2, NECTIN3, NFAM1, NID2, NINJ1, PDGFA, PDGFRB, SELP, SERPINH1, TGFB2, TGFB1, THBS1, THBS2, THY1, TNC, TNFRSF1B, VCAN	
miR-338	ADAM12, ADGRE5, ALPL, APP, BMP6, CCL3, CCN4, CLDN2, COL6A3, CYBA, DAB2, F2R, FOXF2, GLI1, GLIS1, HGF, IL6, INHBA, LAMB3, LAMC2, LUM, NFATC2, NINJ1, PDGFA, THBS2, TNFRSF1B	
miR-450a-5p	COL1A2, COL3A1, COL5A2, HGF, PDGFRB, TGFB2	
miR-29b-3p	ADAMTS2, COL15A1, COL1A1, COL1A2, COL3A1, COL4A1, COL4A2, COL5A1, COL5A2, NID2, PDGFA, VCAN	

Table 3b, continued

ASSOCIATED WITH IN-ACTIVATED NETWORK	Inactivated Causal Network miR-DEG Relationships	
	DEGS ($\text{LOG}_2 > 2, p < 0.05$)	DEGS ($\text{LOG}_2 < -2, p < 0.05$)
miR-2392	–	
miR-200	ADAM12, ALPL, COL1A1, COL1A2, COL3A1, FAT1, FOXF2, IL6, LAMC2, MMP2, SERPINH1, TGFB2, TGFB1, THBS1, VCAM1	
miR-128	IL6	
let-7a-5p	ADAMTS2, COL1A1, COL1A2, COL3A1, COL4A1, COL4A2, COL5A1, COL5A2, IL6, ITGB3, NID2, PDGFA, PXDN, THBS1, TLR4, VCAN	
miR-1	ADAM12, CCL2, IL6, PDGFA	
miR-124-3p	CCL2, PLOD3	
let-7	COL1A1, COL1A2, COL3A1, COL4A1, COL5A2, IL6, ITGB3, THBS1, TLR4	
miR-219a-5p	CD14, TNFRSF1B	
miR-218-5p	COL1A1, LAMB3	
miR-182	FOXF2	
miR-491-5p	MMP2	
MIR99A-LET7C-MIR125B2	CCL2, COL1A1, COL1A2, COL3A1, COL4A1, COL5A2, GLI1, IL6, ITGB3, NOX4, THBS1, TLR4, ADAM12, ADAM8, ADAMTS9, ADGRE5, AMH, APOE, APP, ARRB2, BMP6, CCR1, CCRL2, CLDN2, COL4A2, COL6A3, DPEP1, EMILIN1, F2R, FAT1, FOXF1, HGF, IHH, INHBA, LAMB3, LAMC2, LUM, MFHAS1, NECTIN3, NFAM1, NFATC2, NID2, NINJ1, PCDH18, PDGFA, PDGFRB, SELP, SERPINH1, SMPDL3B, TGFB2, TGFB1, THEMIS2, THY1, TNFRSF12A, TNFRSF1B	
MIR100-LET7A2-MIR125B1	ADAM12, ADAM8, ADAMTS9, ADGRE5, AMH, APOE, APP, ARRB2, BMP6, CCL2, CCR1, CCRL2, CLDN2, COL1A1, COL1A2, COL3A1, COL4A1, COL4A2, COL5A2, COL6A3, DPEP1, EMILIN1, F2R, FAT1, FOXF1, GLI1, HGF, IHH, IL6, INHBA, ITGB3, LAMB3, LAMC2, LUM, MFHAS1, NECTIN3, NFAM1, NFATC2, NID2, NINJ1, NOX4, PCDH18, PDGFA, PDGFRB, SELP, SERPINH1, SMPDL3B, TGFB2, TGFB1, THBS1, THEMIS2, THY1, TLR4, TNFRSF12A, TNFRSF1B	
MIR17HG	ALPL, APP, COL5A1	
MIRLET7	COL1A1, COL1A2, COL5A2, IL6	

Table 4a

Identified miR in activated network indicated through Upstream Regulator analysis (esophageal adenocarcinoma vs. healthy adjacent tissue). miR-DEG targets are divided into upregulated ($\log_2 \text{FC} > 2, p < 0.05$) and downregulated ($\log_2 \text{FC} < 2, p < 0.05$).

Activated Upstream Regulator miR-DEG Relationships		
ASSOCIATED WITH ACTIVATED NETWORK	DEGS ($\text{LOG}_2 > 2, p < 0.05$)	DEGS ($\text{LOG}_2 < -2, p < 0.05$)
miR-223	CCR3, CD180, IL6, POSTN, TGFB1, TLR4	

EAC patients but has yet to be described in tissue biopsy analysis [43]. The moderate overlap between our findings and those already reported serves to validate the dysregulation of previously reported miRs in EAC.

To our knowledge, the remaining 26 miRs identified in this study have yet to be reported concerning EAC compared with normal epithelium and have unknown pathologic implications. These include let-7a-5p, miR-10, miR-124-3p, miR-125b-5p, miR-128, miR-146, miR-155-5p, miR-19, miR-193, miR-204-5p, miR-205-5p, miR-219a-5p, miR-2392, miR-24, miR-28, miR-29, miR-291a-3p, miR-296-5p, miR-29b-3p, miR-30, miR-338, miR-450a-5p, miR-491-5p, miR-8, miR-96-5p, and MIR100-LET7A2-MIR125B1.

4.6. qPCR of DEGS for RNA sequencing validation

We conducted qPCR analysis on 18 genes from our list of 588 DEGs to verify the results of RNA sequencing. The 18 genes were selected based on a literature review. We selected 11 genes that have not been extensively studied in EAC (*PCOLCE*, *SULF1*, *GJA4*, *LUM*, *CDH6*, *GNA12*, *PTGFR*, *F2RL2*, *CTSZ*, *CDC14B*, *KDELR3*, *UGT1A1*) and seven genes previously identified to be associated with EAC: (*CDH11*, *IGFBP7*, *FOXF1*, *CTHRC1*, *TYROBP*, *NFATC2*, *HEYL*). qPCR analysis (Fig. 7) confirmed significant dysregulation in 15 of the 18 selected DEGs in EAC compared to control (*CDH11*, *PCOLCE*, *SULF1*, *GJA4*, *LUM*, *CDH6*, *GNA12*, *F2RL2*, *CTSZ*, *TYROBP*, *KDELR3*, and *UGT1A1*). We compared our results to The Human

Table 4b

Identified microRNAs in inactivated networks indicated through Upstream Regulator analysis (esophageal adenocarcinoma vs. healthy adjacent tissue). miR-DEG targets are divided into upregulated ($\log_2 \text{FC} > 2$, $p < 0.05$) and downregulated ($\log_2 \text{FC} < 2$, $p < 0.05$).

Inactivated Upstream Regulator miR-DEG Relationships		
ASSOCIATED WITH IN-ACTIVATED NETWORK	DEGS ($\text{LOG}_2 > 2$, $p < 0.05$)	DEGS ($\text{LOG}_2 < -2$, $p < 0.05$)
miR-335-3p	ADAMTS2, COL1A1, COL1A2, COL4A1, COL4A2, COL5A1, COL5A2, NID2, PDGFA, VCAN	
miR-338-3p	ADAMTS2, COL1A1, COL1A2, COL4A1, COL4A2, COL5A1, COL5A2, NID2, PDGFA, VCAN	
miR-30c-5p	ADAMTS2, COL1A1, COL1A2, COL4A1, COL4A2, COL5A1, COL5A2, IL6, NID2, PDGFA, VCAN	
miR-450a-5p	COL1A2, COL3A1, COL5A2, HGF, PDGFRB, TGFB2	
miR-29b-3p	ADAMTS2, COL15A1, COL1A1, COL1A2, COL3A1, COL4A1, COL4A2, COL5A1, COL5A2, NID2, PDGFA, VCAN	
miR-2392	–	
let-7a-5p	ADAMTS2, COL1A1, COL1A2, COL3A1, COL4A1, COL4A2, COL5A1, COL5A2, IL6, ITGB3, NID2, PDGFA, PXDN, THBS1, TLR4, VCAN	
miR-124-3p	CCL2, PLOD3	
miR-1	ADAM12, CCL2, IL6, PDGFA	
let-7	COL1A1, COL1A2, COL3A1, COL4A1, COL5A2, IL6, ITGB3, THBS1, TLR4	
miR-29	ADAM12, ADAMTS9, COL1A1, COL1A2, COL3A1, COL4A2, COL5A2, ITGA11, MMP2, PDGFA, PDGFRB, THBS1	
miR-182	FOXF2	
miR-199a-5p	COL1A1, COL4A1, ITGB3, LAMC2, NEDD9	
miR-1-3p	THBS1	
miR-125b-5p	IGFBP3, PCDHB10	
miR-27a-3p	–	
miR-193	CCL2, FAT1	MAPT
miR-155-5p	AMIGO2, CCL18, CCL3, CCL4, IL6	
miR-291a-3p	APP, CCL3, IL6	
miR-205-5p	–	
miR-296-5p	COL1A1, TNC	
miR-8	ADAM12, FAT1, FOXF2, IL6, TGFB2	
miR-335-3p	CCL2, CCL3, IL6, MMP2, TLR4	

Protein Atlas (<https://www.proteinatlas.org/>) to determine whether each respective gene has been reported in esophageal tissue. Of the 15 significantly dysregulated genes confirmed through qPCR, we identified *F2RL2* as “not detected in esophageal tissue” in The Human Protein Atlas but has been shown to relate to overall prognosis in esophageal carcinoma in general [44].

5. Discussion

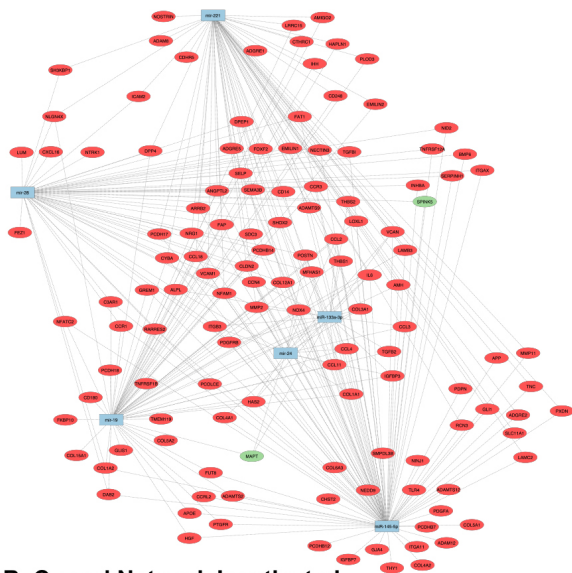
The results of this study delineated 46 unique miRs associated with both activated and inhibited pathways. Seven total miRs were detected to be associated with activated pathways: miR-28, miR-145-5p, miR-19, miR-221, miR-133a-3p, miR-24, and miR-223. Inhibited pathways were influenced by a total of 39 miRs, including miR-149-5p, miR-96-5p, miR-204-5p, miR-10, miR-30, miR-630, miR-338, miR200, miR-128, miR-219a-5p, miR-218-5p, miR-491-5p, MIR100-LET7A2-

MIR125B1, MIR17HG, MIR99A-LET7C-MIR125B2, MIRLET7, miR-29, miR-199a-5p, miR-1-3p, miR-125b-5p, miR-27a-3p, miR-193, miR-155-5p, miR-291a-3p, miR-205-5p, miR-296-5p, miR-8, miR-146, miR-335-3p, miR-30c-5p, miR-338-3p, miR-450a-5p, miR-29b-3p, miR-2392, let-7a-5p, miR-1, miR-124-3p, let-7, and miR-182. We found no miRs with activity in both activated and inhibited pathways. Comparative analysis revealed that 11 miRs were found to regulate inactivated pathways in both causal network and upstream regulator analyses (miR-335-3p, miR-30c-5p, miR-338-3p, miR-450a-5p, miR-29b-3p, miR-2392, let-7a-5p, miR-1, miR-124-3p, let-7, and miR-182). Further, the dysregulation of DEG expression confirmed through qPCR provides insight into the potential oncogenic role of miRs in EAC. We verified mRNA expression in esophageal tissue for genes *CDH11*, *PCOLCE*, *SULF1*, *GJA4*, *LUM*, *CDH6*, *GNA12*, *CTS2*, *TYROBP*, *KDELR3*, and *UGT1A1*. We found that the protein expression of *F2RL2* has not been reported in The Human

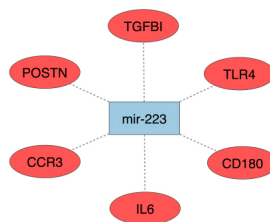
miR-Gene Relationships Identified Through Ingenuity Pathway Analysis

miR Targets

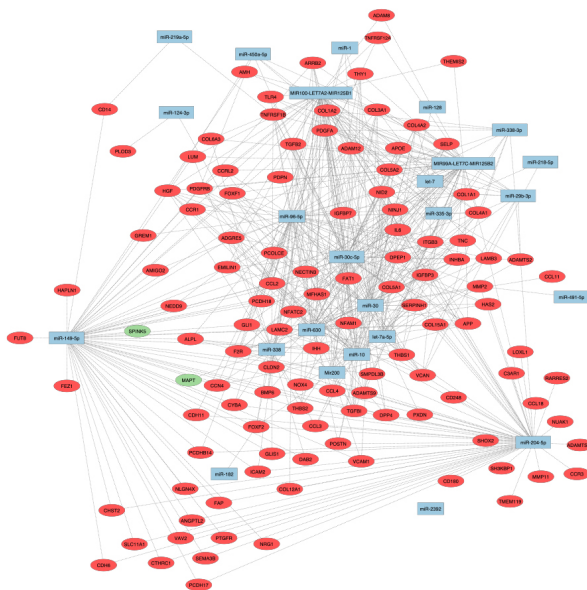
A. Causal Network Activated



C. Upstream Regulator Activated



B. Causal Network Inactivated



D. Upstream Regulator Inactivated

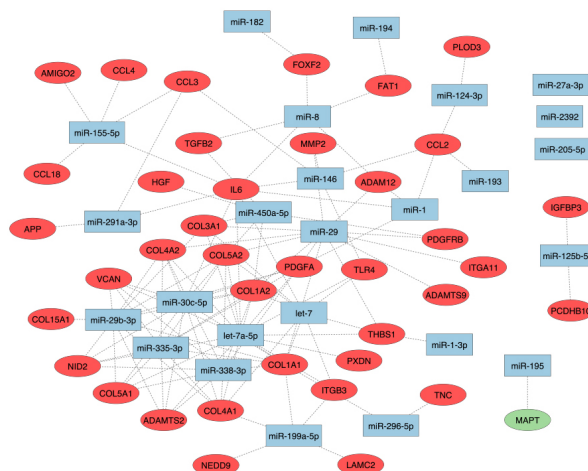


Fig. 6. miRs identified through IPA analysis (esophageal adenocarcinoma vs. healthy adjacent tissue). A) Causal Network Activated; B) Causal Network Inactivated; C) Upstream Regulator Activated; D) Upstream Regulator Inactivated. Red circles: upregulated genes, green circles: downregulated genes, blue squares: microRNAs, dotted line: predicted miR-gene interaction. Nodes without predicted activity were removed. Image generated using Cytoscape (<https://cytoscape.org/>).

Protein Atlas but has been associated with prognosis in esophageal carcinoma [44]. This bolsters the notion that aberrant expression of *F2RL2* is associated with EAC pathogenesis and thus warrants future investigation.

In this study, we identified significant upregulation in

the expression of genes and gene pathways that play a critical role in mediating and maintaining the extracellular matrix and cellular adhesion. Disorganization of the extracellular matrix (ECM) plays an essential role in tumorigenesis. In healthy tissues, the ECM comprises

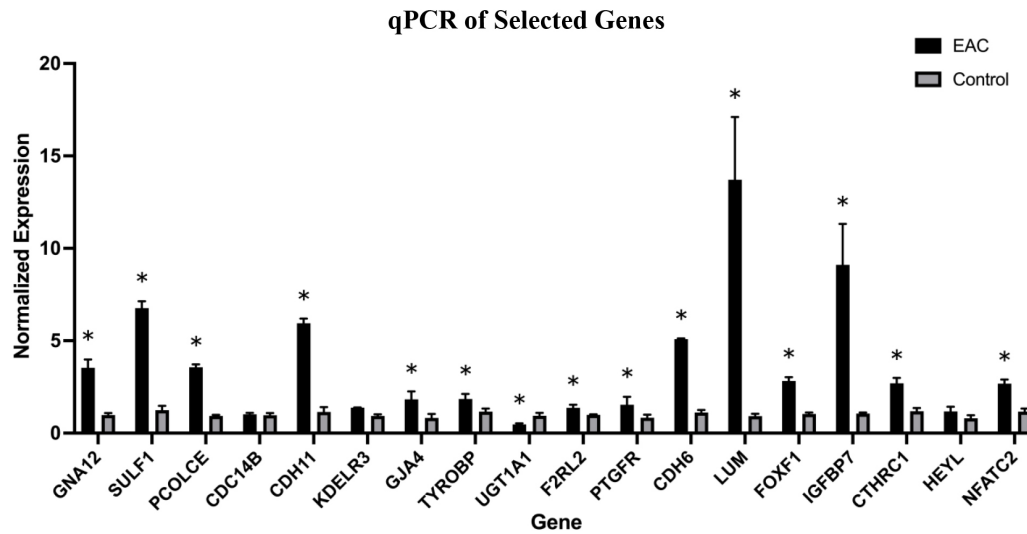


Fig. 7. Graph representing normalized expression of qPCR product for selected genes ($n = 18$) in esophageal adenocarcinoma tissue vs. control to validate results of RNA sequencing. (Black = esophageal adenocarcinoma; grey = healthy control tissue. Significant difference ($p < 0.05$) denoted with asterisk: *).

scaffolded collagen, non-collagen, and proteoglycan molecules that serve various functions in cell signaling and structural support [45]. Tumorigenic stimuli disrupt the normal function and makeup of the ECM through extensive modification that favorably supports rapidly expanding dysplastic cell lines [46]. Additionally, alteration in the makeup of ECM proteins appears to increase cell migration to favor metastasis [46,47]. In the present study, multiple genes and gene pathways related to the ECM were identified as significantly expressed. One crucial component of the ECM is the proteoglycan Lumican (*LUM*) which functions to provide structural organization of extracellular collagen fibrils [48]. Dysregulation of *LUM* has been identified to influence the progression of multiple cancers, including gastric, breast, and colon [49,50,51]. In gastric cancer, increased *LUM* expression has been associated with poorer histologic evaluation, metastasis, and worsened overall survival [52]. Our current data support an increased expression of *LUM* in EAC tissue compared to control. We identified significant Lumican overexpression in RNA-sequencing and qPCR methods of analysis. We also found Lumican to be a highly connected hub gene in hub gene analysis, displaying overlap between both methodologies. Further, GO Term enrichment identified *LUM* in the highly enriched process of Collagen Fibril Organization. Together, these findings suggest its importance in the protein-protein networks underlying EAC pathophysiology. miR-28, associated with inactivated networks, appears to play

a role in the upregulation of *LUM* expression. miR-28 expression has been shown to promote carcinogenesis in gastric tissue and in non-small cell lung cancer, both through *PTEN*-mediated pathways that promote cell proliferation and/or invasion [53,54]. In EAC, miR-28-mediated increased expression of *LUM* may confer a tendency for transitional tissues to become malignant through similar mechanisms which ultimately promote cell proliferation and invasion by modification of the ECM. The pathway by which this occurs is of interest but requires further study to be fully characterized.

Procollagen C-endopeptidase enhancer (*PCOLCE*) is another gene found within the separate but highly related collagen biosynthetic process GO Term that we found to be significantly upregulated in EAC samples compared to the control. Members of the *PCOLCE* family of proteins engage in enhancing the function of procollagen C proteinases in the construction of collagen fibrils [55]. Dysregulation of this mechanism can lead to carcinogenesis and has been documented to be related to increased *PCOLCE* levels in multiple cancers. According to an analysis of The Cancer Genome Atlas, increased expression of *PCOLCE* can confer poor prognosis in esophageal cancers, although the frequency in which *PCOLCE* becomes dysregulated is relatively low [56]. Additionally, The Cancer Genome Atlas groups all types of esophageal cancers together, making its exact relationship to EAC difficult to identify. In gastric cancer, increased expression of *PCOLCE* was shown to relate directly to increased immunoinfli-

trate and is associated with unfavorable prognosis [57]. In addition to its significant upregulation, we identified *PCOLCE* to be a highly connected hub gene in our samples, providing evidence that it plays a vital role in the EAC carcinogenic process. We found that *PCOLCE* was influenced by miR-133a-3p in activated networks by causal network analysis. In esophageal squamous cell carcinoma, miR-133a-3p has been identified to suppress the expression of collagen type 1 alpha 1, leading to decreased proliferation and migration [58]. In a variety of other cancers, members of the miR-133a family of microRNAs have been described to play a variety of roles and participate in a range of cellular signaling pathways, though the bulk of evidence suggests miR-133a-related species protect against carcinogenesis [59]. To the best of our knowledge, no relationship between *PCOLCE* and miR-133a-3p has been established in the literature. However, it appears that miR-133a-3p dysregulation leads, either directly or indirectly, to an increase in *PCOLCE* expression and ultimately influences the construction of collagen fibrils. Our results suggest an important role for this relationship in EAC development and deserves further study to delineate the exact mechanism by which this occurs.

We also identified the most significantly enriched pathway in our samples as cell adhesion. Within this pathway, we uncovered that cadherin 11 (*CDH11*) is significantly upregulated. *CDH11* has a well-defined role in carcinogenesis and is frequently cited as tumor-suppressive, achieving this function through promoting apoptosis by increasing promotor methylation. Upregulation of *CDH11* has been shown to reduce tumorigenicity of cell lines, including in those of esophageal squamous cell carcinoma [60,61]. In this study, we identified that *CDH11* was part of a group of highly connected hub genes identified through both cytoHubba and MCODE analysis, suggesting its importance as a gene related to the underlying pathophysiology in EAC. We further discovered through causal network analysis that the increase in *CDH11* observed in this study is related to inactivated networks downstream of miR-96-5p. Application of a conventional understanding of the role of *CDH11* would suggest that increased expression should correlate with decreased incidence of carcinogenesis, and this may be related to the staging of our samples, which we did not include in our analysis. Increased *CDH11* may confer more favorable histologic staging of EAC samples, though this relationship is not yet studied and serves as an interesting question to be answered in future analysis.

Furthermore, heparan sulfate proteoglycans (HSPGs) within the ECM serve as co-receptors for various ECM

ligands, including cytokines, chemokines, and growth factors. HSPGs undergo extensive enzymatic modification, leading to a diversity of binding sites to facilitate cell-surface signaling. 6-O-endosulfatases are one class of HSPG-modifying enzymes that includes sulfatase-1 (*SULF1*) [62]. *SULF1* dysregulation has been attributed to both tumorigenic and tumor-suppressive roles in the literature, suggesting a complicated network of interactions between many of its associated modulators. As a tumorigenic focus, elevated *SULF1* expression has been associated with poor prognosis in hepatocellular carcinoma by promoting the progression of EMT (epithelial-mesenchymal transition) and tumor invasion. In this capacity, *SULF1* is thought to upregulate transforming growth factor beta ($TGF\beta$)-induced transcription through the SMAD/ $TGF\beta$ pathway by promoting $TGF\beta$ release from the receptor $TGF\beta R3$ [63]. Increased $TGF\beta$ signaling is well-known to promote EMT, making this signaling pathway interesting in the study of EAC [64]. Interestingly, we identified *SULF1* as significantly upregulated in EAC in both qPCR and RNA-sequencing studies. Beyond this, *SULF1* was identified as an important, highly connected hub gene through cytoHubba DMNC analysis. IPA analysis revealed that, in our experiment, *SULF1* expression was influenced by miR-193, which was associated with inactivated pathways upstream of its targets. The miR-193 family of microRNAs is understood to provide tumor suppressive effects in a variety of cancers [65]. In EAC, it is likely that miR-193 dysregulation increases the expression of *SULF1* during carcinogenesis and expedites the metaplastic process by promoting EMT, ultimately leading to EAC development from transitional tissues. Although the exact mechanism of this is unclear, this relationship is of great interest and should be explored.

In this study, we further identified significant upregulation in the expression of genes and gene pathways that play a critical role in mediating inflammation. Chronic inflammatory stimulus within the esophageal mucosa is a well-established risk factor for developing EAC by promoting cell proliferation, growth, and migration [66,67,68]. The inflammatory microenvironment is also marked by the recruitment of numerous immune-associated cells, including T-cells, Natural Killer cells, and macrophages [69]. In multiple cancers, including EAC, the phenotypic makeup of immune cells within the inflammatory microenvironment has been shown to correlate with tumorigenicity [70, 71]. Of these cells, macrophages recruited to the area of inflammation promote the formation of extracellular matrix, perform phagocytosis, and provide posi-

tive feedback for further cell recruitment through cytokine/chemokine release. Macrophage infiltration into the affected tissue subsequently follows with polarization into subtypes that specialize in different features [72,73]. For example, circulating macrophages recruited to the site of early tumor formation polarize into primarily M1 tumor-associated macrophages (TAMs). M1 TAMs promote an anti-tumorigenic microenvironment in part through enhancing inflammation and antigen presentation [72,74,75]. Over time, macrophages polarize into predominantly M2 TAMs due to exposure to inflammatory cytokines [73]. M2 macrophage predominance has been associated with pro-tumor activity and resistance to anti-tumor therapy [73,76,77,78,79,80]. In esophageal squamous carcinoma, M2 macrophage infiltration has been shown to promote tumor cell expansion, invasion, and migration by suppressing the anti-tumorigenic activities of neighboring cells [81]. In EAC, M2 macrophage polarization appears to occur in response to tumor up-regulation of Th2 pathways, leading to increased IL-4 and IL-13 [82]. Like other cancers, EAC treatment success is partially dictated by relatively low levels of infiltrating macrophages compared to other immune constituents [83]. Taken together, M2 macrophages may become an attractive target in the emerging treatment of EAC. One putative marker of tumor-associated macrophages is TREM2 [84,85,86]. TREM2 signaling is complex and involves a variety of modulating proteins, such as TYRO protein tyrosine kinase-binding protein (*TYROBP*), one of the central hub genes identified during this study. *TYROBP* expression has been identified to correlate with M2 macrophage infiltration and prognosis in ESCC [87]. In addition, the TREM2-*TYROBP* axis has been implicated through small interfering RNA experiments to promote EAC development [88]. In the present study, we identified a significant increase in *TYROBP* through RNA sequencing and qPCR. In conjunction, we identified the miR cluster MIR100-LET7A2-MIR125B1 to influence inactivated networks upstream of the increased expression of *TYROBP*. This miR-cluster has been identified to regulate the magnitude of transforming growth factor β signaling in human carcinomas [89], a potent regulator of macrophage polarization [90]. Taken together, the pathways inactivated by MIR100-LET7A2-MIR125B1 induce an immuno-modulating increase in *TYROBP* expression that may contribute to M2-polarization and ultimately contribute to pro-tumorigenic changes within the inflammatory microenvironment of EAC tissues and its precursors. Although the exact mechanism of

this is unclear, how *TYROBP* and MIR100-LET7A2-MIR125B1 promote tumorigenesis in EAC is worthy of future study.

6. Conclusion

Correlation of IPA, qPCR, and RNA-sequencing analysis reveals a novel profile of miRs that occur in the setting of EAC. miRs regulating upregulated genes were found to be associated with inhibited pathways through IPA. miRs associated with downregulated genes were discovered to be activated in IPA analysis. While miR influence on gene expression is likely complex, this association bolsters our hypothesis that miRs regulate gene expression and contribute to EAC pathogenesis. Based on these findings, it is evident that the miRs discovered in this study may be used as biomarkers for EAC. However, comparative analysis and correlation with BE tissues will be essential in establishing diagnostic miR profiles.

Further, significantly increased mRNA expression of *CDH11*, *PCOLCE*, *SULF1*, *GJA4*, *LUM*, *CDH6*, *GNA12*, *F2RL2*, *CTSZ*, *TYROBP*, and *KDELR3* and decreased expression of *UGT1A1* in EAC tissues suggest that aberrant expression of specific genes play a role in EAC pathogenesis that may guide future research efforts.

In this study, we also identified 32 candidate hub genes associated with EAC and identified the top 10 significantly enriched GO Terms based on our panel of dysregulated genes, which included processes involved in cell adhesion, extracellular matrix, inflammation, cell signaling and cell migration, amongst others.

Limitations

There are a few notable limitations to this study that warrant further investigation. For one, we limited our sample size to four patients. Beyond this, we did not include samples of Barrett's esophagus for comparative analysis. In addition, we did not include histology grading, staging information, or immunohistochemical analysis of sample tissues to evaluate for protein expression. Despite these limitations, this study delineated novel miRs, reported for the first time, in association with aberrant genes detected in EAC.

Acknowledgments

No funding.

Author contributions

Conception: Kalyana Nandipati, MD, and Vikrant Rai.

Interpretation or analysis of data: Ryan Corlett, Vikrant Rai, and Swati Agrawal.

Preparation of the manuscript: Ryan Corlett, Vikrant Rai, Sydney Scheel, and Charles Button.

Revision for important intellectual content: Ryan Corlett, Kalyana Nandipati, MD, and Vikrant Rai.

Supervision: Kalyana Nandipati, MD, and Vikrant Rai.

Conflict of interest

The authors have declared no conflict of interest.

Data availability

IPA predicted miRs, qPCR, and comparative analysis of genes available in Supplemental File 1. The RNA sequences generated and analyzed during the current study are available in the NCBI Sequence Read Archive repository, <https://www.ncbi.nlm.nih.gov/bioproject/?term=PRJNA945944>.

Glossary of Abbreviations

Abbreviation	Definition
DEG	Differentially Expressed Gene
EAC	Esophageal adenocarcinoma
ECM	Extracellular Matrix
EMT	Epithelial-Mesenchymal Transition
FC	Fold Change
FDR	False Discovery Rate
FPKM	Fragments Per Kilobase of transcript per Million mapped reads
GO	Gene Ontology
GPCR	G-Protein Coupled Receptor
HSPG	Heparan sulfate proteoglycan
IPA	Ingenuity Pathway Analysis
miR	microRNA
mRNA	Messenger RNA
PPI	Protein-Protein Interaction
qPCR	Real-time polymerase chain reaction
RNA	Ribonucleic acid
STRING	Search Tool for Retrieval of Interacting Genes
TAM	Tumor-Associated Macrophage

TGF β	transforming growth factor beta
TPM	Transcripts Per Kilobase Million
UNMC	University of Nebraska Medical Center

Supplementary data

The supplementary files are available to download from <http://dx.doi.org/10.3233/CBM-230170>.

References

- [1] D.J. Uhlenhopp, E.O. Then, T. Sunkara and V. Gaduputi, Epidemiology of esophageal cancer: update in global trends, etiology and risk factors, *Clinical Journal of Gastroenterology* **13** (2020), 1010–1021.
- [2] M.J. Domper Arnal, Á. Ferrández Arenas and Á. Lanás Arbeloa, Esophageal cancer: Risk factors, screening and endoscopic treatment in Western and Eastern countries, *World Journal of Gastroenterology* **21** (2015), 7933–43.
- [3] R.L. Siegel, K.D. Miller, N.S. Wagle and A. Jemal, Cancer statistics, 2023, *CA: A Cancer Journal for Clinicians* **73** (2023), 17–48.
- [4] H. He, et al., Trends in the incidence and survival of patients with esophageal cancer: A SEER database analysis, *Thoracic Cancer* **11** (2020), 1121–1128.
- [5] Z. Haiyu, et al., Incidence and Survival Changes in Patients with Esophageal Adenocarcinoma during 1984–2013, *BioMed Research International* (2019), 7431850.
- [6] E. Corona, et al., Trends in Esophageal Cancer Mortality and Stage at Diagnosis by Race and Ethnicity in the United States, *Cancer Causes Control* **32** (2021), 883–894.
- [7] M.R. Gillespie, V. Rai, S. Agrawal and K.C. Nandipati, The Role of Microbiota in the Pathogenesis of Esophageal Adenocarcinoma, *Biology (Basel)* **10** (2021).
- [8] J.E. Bradner, D. Hnisz and R.A. Young, Transcriptional Addiction in Cancer, *Cell* **168** (2017), 629–643.
- [9] G. di Leva, M. Garofalo and C.M. Croce, MicroRNAs in cancer, *Annual Review of Pathology* **9** (2014), 287–314.
- [10] Y.S. Lee and A. Dutta, MicroRNAs in cancer, *Annual Review of Pathology* **4** (2009), 199–227.
- [11] W.C.S. Cho, OncomiRs: the discovery and progress of microRNAs in cancers, *Molecular Cancer* **6** (2007), 60.
- [12] A. Vishnoi and S. Rani, miRNA Biogenesis and Regulation of Diseases: An Updated Overview, *Methods in Molecular Biology* **2595** (2023), 1–12.
- [13] Z. Ali Syeda, et al., Regulatory Mechanism of MicroRNA Expression in Cancer, *International Journal of Molecular Sciences* **21** (2020).
- [14] M.V. Iorio and C.M. Croce, MicroRNA dysregulation in cancer: diagnostics, monitoring and therapeutics. A comprehensive review, *EMBO Molecular Medicine* **4** (2012), 143–59.
- [15] M.D. Jansson and A.H. Lund, MicroRNA and cancer, *Molecular Oncology* **6** (2012), 590–610.
- [16] M. Budakoti, et al., Micro-RNA: The darkhorse of cancer, *Cellular Signaling* **83** (2021), 109995.
- [17] J.L.V. Maag, et al., Novel Aberrations Uncovered in Barrett's Esophagus and Esophageal Adenocarcinoma Using Whole Transcriptome Sequencing, *Molecular Cancer Research* **15** (2017), 1558–1569.

- [18] J.L. Petrick, et al., Circulating MicroRNAs in Relation to Esophageal Adenocarcinoma Diagnosis and Survival, *Digestive Diseases and Sciences* **66** (2021), 3831–3841.
- [19] D. Matsui et al., Primary tumor microRNA signature predicts recurrence and survival in patients with locally advanced esophageal adenocarcinoma, *Oncotarget* **7** (2016), 81281–81291.
- [20] H. Yang, et al., MicroRNA expression signatures in Barrett's esophagus and esophageal adenocarcinoma, *Clinical Cancer Research* **15** (2009), 5744–52.
- [21] A. Feber, et al., MicroRNA expression profiles of esophageal cancer, *The Journal of Thoracic and Cardiovascular Surgery* **135** (2008), 255–60; discussion 260.
- [22] J. Drahos, et al., MicroRNA Profiles of Barrett's Esophagus and Esophageal Adenocarcinoma: Differences in Glandular Non-native Epithelium, *Cancer Epidemiology, Biomarkers & Prevention* **25** (2016), 429–37.
- [23] S. Andrews, FastQC: A Quality Control Tool for High Throughput Sequence Data, (2015). Available online at: <http://www.bioinformatics.babraham.ac.uk/projects/fastqc>.
- [24] A. Dobin, et al., STAR: ultrafast universal RNA-seq aligner, *Bioinformatics* **29** (2013), 15–21.
- [25] B. Li and C.N. Dewey, RSEM: accurate transcript quantification from RNA-Seq data with or without a reference genome, *BMC Bioinformatics* **12** (2011), 323.
- [26] Y. Benjamini and Y. Hochberg, Controlling the False Discovery Rate: A Practical and Powerful Approach to Multiple Testing, *Journal of the Royal Statistical Society Series B (Methodological)* **57** (1995), 289–300.
- [27] P. Langfelder, P.S. Mischel and S. Horvath, When is hub gene selection better than standard meta-analysis? *PLoS One* **8** (2013), e61505.
- [28] C.H. Chin, et al., cytoHubba: identifying hub objects and sub-networks from complex interactome, *BMC Systems Biology* **8**(Supplement 4) (2014), S11.
- [29] H. Ma, et al., Identifying of biomarkers associated with gastric cancer based on 11 topological analysis methods of CytoHubba, *Scientific Reports* **11** (2021), 1331.
- [30] G.D. Bader and C.W.V Hogue, An automated method for finding molecular complexes in large protein interaction networks, *BMC Bioinformatics* **4** (2003), 2.
- [31] M. Amin and A.K. Lam, Current perspectives of mi-RNA in oesophageal adenocarcinoma: Roles in predicting carcinogenesis, progression and values in clinical management, *Experimental Molecular Pathology* **98** (2015), 411–8.
- [32] X. Wu, et al., MicroRNA expression signatures during malignant progression from Barrett's esophagus to esophageal adenocarcinoma, *Cancer Prevention Research (Philadelphia)* **6** (2013), 196–205.
- [33] J. Matsuzaki and H. Suzuki, Circulating microRNAs as potential biomarkers to detect transformation of Barrett's oesophagus to oesophageal adenocarcinoma, *BMJ Open Gastroenterology* **4** (2017), e000160.
- [34] C.H. Lai, et al., Study on miRNAs in Pan-Cancer of the Digestive Tract Based on the Illumina HiSeq System Data Sequencing, *BioMed Research International* (2019), 8016120.
- [35] L. Zhang, et al., c-Myb facilitates immune escape of esophageal adenocarcinoma cells through the miR-145-5p/SPOP/PD-L1 axis, *Clinical and Translational Medicine* **11** (2021), e464.
- [36] U. Warnecke-Eberz, et al., Exosomal onco-miRs from serum of patients with adenocarcinoma of the esophagus: comparison of miRNA profiles of exosomes and matching tumor, *Tumor Biology* **36** (2015), 4643–53.
- [37] S. Tang, et al., Stratification of Digestive Cancers with Different Pathological Features and Survival Outcomes by MicroRNA Expression, *Scientific Reports* **6** (2016), 24466.
- [38] J. Matsuzaki and H. Suzuki, Role of MicroRNAs-221/222 in Digestive Systems, *Journal of Clinical Medicine* **4** (2015), 1566–77.
- [39] A.K. Eichelmann, et al., Mutant p53 Mediates Sensitivity to Cancer Treatment Agents in Oesophageal Adenocarcinoma Associated with MicroRNA and SLC7A11 Expression, *International Journal of Molecular Sciences* **22** (2021).
- [40] C. Zhan, et al., Landscape of expression profiles in esophageal carcinoma by The Cancer Genome Atlas data, *Diseases of the Esophagus: official journal of the International Society for Diseases of the Esophagus/I.S.D.E* **29** (2016), 920–928.
- [41] P.S. Plum, et al., Upregulation of miR-17-92 cluster is associated with progression and lymph node metastasis in oesophageal adenocarcinoma, *Scientific Reports* **9** (2019), 12113.
- [42] C.M. Smith, et al., miR-200 family expression is downregulated upon neoplastic progression of Barrett's esophagus, *World Journal of Gastroenterology* **17** (2011), 1036–44.
- [43] A.A. van Zweeken, et al., The prognostic impact of circulating miRNAs in patients with advanced esophagogastric cancer during palliative chemotherapy, *Cancer Treatment and Research Communications* **27** (2021), 100371.
- [44] C. Li, et al., Identification of an Immune-Related Gene Signature Associated with Prognosis and Tumor Microenvironment in Esophageal Cancer, *BioMed Research International* **2022** (2022), 7413535.
- [45] C. Frantz, K.M. Stewart and V.M. Weaver, The extracellular matrix at a glance, *Journal of Cell Science* **123** (2010), 4195–200.
- [46] J. Winkler, A. Abisoye-Ogunniyan, K.J. Metcalf and Z. Werb, Concepts of extracellular matrix remodeling in tumour progression and metastasis, *Nature Communications* **11** (2020), 5120.
- [47] J.M. Powers, J.C. Roberts and R.G. Craig, Surface failure of commercial and experimental restorative resins, *Journal of Dental Research* **55** (1976), 432–6.
- [48] S. Chakravarti, et al., Lumican regulates collagen fibril assembly: skin fragility and corneal opacity in the absence of lumican, *The Journal of Cell Biology* **141** (1998), 1277–86.
- [49] X. Wang, et al., Cancer-associated fibroblast-derived Lumican promotes gastric cancer progression via the integrin β 1-FAK signaling pathway, *International Journal of Cancer* **141** (2017), 998–1010.
- [50] K. Karamanou, M. Franchi, D. Vynios and S. Brézillon, Epithelial-to-mesenchymal transition and invadopodia markers in breast cancer: Lumican a key regulator, *Seminars in Cancer Biology* **62** (2020), 125–133.
- [51] A. Radwanska, et al., Overexpression of lumican affects the migration of human colon cancer cells through up-regulation of gelsolin and filamentous actin reorganization, *Experimental Cell Research* **318** (2012), 2312–23.
- [52] E.M. Giatagana, et al., Lumican in Carcinogenesis-Revisited, *Biomolecules* **11** (2021).
- [53] F. Cui, Q. Zhou, K. Xiao and H. Qian, MicroRNA-28 promotes the proliferation of non-small-cell lung cancer cells by targeting PTEN, *Molecular Medicine Reports* **21** (2020), 2589–2596.
- [54] L. Li, et al., MicroRNA-28 promotes cell proliferation and invasion in gastric cancer via the PTEN/PI3K/AKT signaling pathway, *Molecular Medicine Reports* **17** (2018), 4003–4010.
- [55] B.M. Steiglit, et al., Procollagen C proteinase enhancer 1 genes are important determinants of the mechanical properties

- and geometry of bone and the ultrastructure of connective tissues, *Molecular and Cellular Biology* **26** (2006), 238–49.
- [56] H. Gao and Q. Li, A pan-cancer analysis of the oncogenic role of procollagen C-endopeptidase enhancer (PCOLCE) in human, *Medicine* **101** (2022), e32444.
- [57] A. Xiang, et al., PCOLCE Is Potent Prognostic Biomarker and Associates With Immune Infiltration in Gastric Cancer, *Frontiers in Molecular Biosciences* **7** (2020), 544895.
- [58] Y. Yin, et al., miR-133a-3p suppresses cell proliferation, migration, and invasion and promotes apoptosis in esophageal squamous cell carcinoma, *Journal of Cellular Physiology* **234** (2019), 12757–12770.
- [59] Y.T. Hua, W.X. Xu, H. Li and M. Xia, Emerging roles of MiR-133a in human cancers, *Journal of Cancer* **12** (2021), 198–206.
- [60] L. Li, et al., The human cadherin 11 is a pro-apoptotic tumor suppressor modulating cell stemness through Wnt/ β -catenin signaling and silenced in common carcinomas, *Oncogene* **31** (2012), 3901–12.
- [61] X. Chen, et al., Research progress in the role and mechanism of Cadherin-11 in different diseases, *Journal of Cancer* **12** (2021), 1190–1199.
- [62] E. Hammond, A. Khurana, V. Shridhar and K. Dredge, The Role of Heparanase and Sulfatases in the Modification of Heparan Sulfate Proteoglycans within the Tumor Microenvironment and Opportunities for Novel Cancer Therapeutics, *Frontiers in Oncology* **4** (2014), 195.
- [63] R. Dhanasekaran, et al., Activation of the transforming growth factor- β /SMAD transcriptional pathway underlies a novel tumor-promoting role of sulfatase 1 in hepatocellular carcinoma, *Hepatology* **61** (2015), 1269–83.
- [64] Y. Hao, D. Baker and P.T. Dijke, TGF- β -Mediated Epithelial-Mesenchymal Transition and Cancer Metastasis, *International Journal of Molecular Sciences* **20** (2019).
- [65] M. Khordadmehr, R. Shahbazi, S. Sadreddini and B. Baradaran, miR-193: A new weapon against cancer, *Journal of Cellular Physiology* **234** (2019), 16861–16872.
- [66] T. Fujimura, et al., Inflammation-related carcinogenesis and prevention in esophageal adenocarcinoma using rat duodenoesophageal reflux models, *Cancers (Basel)* **3** (2011), 3206–24.
- [67] M.M.M. Abdel-Latif, S. Duggan, J.V. Reynolds and D. Kelleher, Inflammation and esophageal carcinogenesis, *Current Opinion in Pharmacology* **9** (2009), 396–404.
- [68] M.E. Kavanagh, et al., The esophagitis to adenocarcinoma sequence; the role of inflammation, *Cancer Letters* **345** (2014), 182–9.
- [69] L.M. Schiffmann, et al., Tumor Microenvironment of Esophageal Cancer, *Cancers (Basel)* **13** (2021).
- [70] F. Pagès, et al., Immune infiltration in human tumors: a prognostic factor that should not be ignored, *Oncogene* **29** (2010), 1093–102.
- [71] R. Haddad, et al., Tumor Lymphocyte Infiltration Is Correlated with a Favorable Tumor Regression Grade after Neoadjuvant Treatment for Esophageal Adenocarcinoma, *Journal of Personalized Medicine* **12** (2022).
- [72] C.D. Mills, M1 and M2 Macrophages: Oracles of Health and Disease, *Critical Reviews in Immunology* **32** (2012), 463–88.
- [73] A.J. Boutillier and S.F. ElSawa, Macrophage Polarization States in the Tumor Microenvironment, *International Journal of Molecular Sciences* **22** (2021).
- [74] S.D. Jayasingam, et al., Evaluating the Polarization of Tumor-Associated Macrophages Into M1 and M2 Phenotypes in Human Cancer Tissue: Technicalities and Challenges in Routine Clinical Practice, *Frontiers in Oncology* **9** (2019), 1512.
- [75] X. Zheng, et al., Redirecting tumor-associated macrophages to become tumoricidal effectors as a novel strategy for cancer therapy, *Oncotarget* **8** (2017), 48436–48452.
- [76] A. Mantovani, et al., Macrophage polarization: tumor-associated macrophages as a paradigm for polarized M2 mononuclear phagocytes, *Trends in Immunology* **23** (2002), 549–55.
- [77] F.J. van Dalen, et al., Molecular Repolarisation of Tumour-Associated Macrophages, *Molecules* **24** (2018).
- [78] F. Pantano, et al., The role of macrophages polarization in predicting prognosis of radically resected gastric cancer patients, *Journal of Cellular and Molecular Medicine* **17** (2013), 1415–21.
- [79] C. Yang, et al., Increased drug resistance in breast cancer by tumor-associated macrophages through IL-10/STAT3/bcl-2 signaling pathway, *Medical Oncology* **32** (2015), 352.
- [80] R. Hughes, et al., Perivascular M2 Macrophages Stimulate Tumor Relapse after Chemotherapy, *Cancer Research* **75** (2015), 3479–91.
- [81] X. Yuan, et al., Tumor-associated macrophage polarization promotes the progression of esophageal carcinoma, *Aging* **13** (2020), 2049–2072.
- [82] J. Gao, et al., Infiltration of alternatively activated macrophages in cancer tissue is associated with MDSC and Th2 polarization in patients with esophageal cancer, *PLoS One* **9** (2014), e104453.
- [83] S.J.M. Hoefnagel, et al., Identification of Novel Molecular Subgroups in Esophageal Adenocarcinoma to Predict Response to Neo-Adjuvant Therapies, *Cancers (Basel)* **14** (2022).
- [84] K. Nakamura and M.J. Smyth, TREM2 marks tumor-associated macrophages, *Signal Transduction and Targeted Therapy* **5** (2020), 233.
- [85] M. Binnewies, et al., Targeting TREM2 on tumor-associated macrophages enhances immunotherapy, *Cell Reports* **37** (2021), 109844.
- [86] A. Deczkowska, A. Weiner and I. Amit, The Physiology, Pathology, and Potential Therapeutic Applications of the TREM2 Signaling Pathway, *Cell* **181** (2020), 1207–1217.
- [87] J. Yao, et al., Development and Validation of a Prognostic Gene Signature Correlated With M2 Macrophage Infiltration in Esophageal Squamous Cell Carcinoma, *Frontiers in Oncology* **11** (2021), 769727.
- [88] S.P. Duggan, et al., siRNA Library Screening Identifies a Drug-gable Immune-Signature Driving Esophageal Adenocarcinoma Cell Growth, *Cellular and Molecular Gastroenterology and Hepatology* **5** (2018), 569–590.
- [89] P. Papoutsoglou, et al., The noncoding MIR100HG RNA enhances the autocrine function of transforming growth factor β signaling, *Oncogene* **40** (2021), 3748–3765.
- [90] F. Zhang, et al., TGF- β induces M2-like macrophage polarization via SNAIL-mediated suppression of a pro-inflammatory phenotype, *Oncotarget* **7** (2016), 52294–52306.